PHYSICAL REVIEW B **79**, 041403(R) (2009)

Thermal photocatalytic generation of H_2 over $CuAlO_2$ nanoparticle catalysts in H_2O

John R. Smith,[1,2] Thomas H. Van Steenkiste,[1] and Xiao-Gang Wang[1]
[1]*Hydrogen Generation Inc., Birmingham, Michigan 48009, USA*
[2]*Department of Materials Science and Engineering, University of Michigan, Ann Arbor, Michigan 48109, USA*

(Received 16 October 2008; published 16 January 2009)

It is becoming increasingly important to find renewable carbon-free energy sources. Harnessing the relatively large potential of solar radiation is currently the subject of considerable research. We have found a relatively strong thermal activation process for photocatalytic water splitting. Our measurements indicate an order of magnitude increase in hydrogen generation rates for a temperature rise of 50 °C, suggesting an approach to practical efficiencies. Generation rates are stable over time. This process, which makes use of ultraviolet, visible, and infrared components of the solar spectrum, is analyzed via first-principles computations.

DOI: 10.1103/PhysRevB.79.041403 PACS number(s): 82.50.Hp, 81.16.Hc, 68.43.Vx, 82.65.+r

Producing hydrogen via solar radiation has long[1] been a goal. Fujishima and Honda[2] showed that a TiO_2 electrode in a galvanic cell can absorb sunlight to promote H_2 production. More recently, a photocatalytic approach to produce H_2 via water splitting from ultraviolet and even visible sunlight has evolved.[3–5] Despite considerable progress, desired solar energy to H_2 fuel energy efficiencies have yet to be obtained, and processes are not always stable over time. At the same time, solar thermal[6–8] energy is being employed to produce H_2 at operating temperatures of 700–2500 °C. The challenge there is to find materials that survive high temperatures and often aggressive chemical environments.

We have found promising results by combining thermal and photocatalytic effects to produce H_2. The goal is a stable process, producing H_2 generation rates high enough to be of practical interest within a noncorrosive environment and with lower operating temperatures than those of solar thermal processes. We investigated this thermal-photocatalytic process via a dispersion of $CuAlO_2$ catalyst nanoparticles in water and sunlight. A schematic of our apparatus is shown in Fig. 1. Natural sunlight is the source of solar radiation and the axis of the cylindrical hydrogen generation container is aligned with the sun. In this first experiment, solar heating is supplemented by electrical resistance heating to increase the water temperature. There are no electrodes in the water and hence no potential for ion currents leading to photocorrosion. In fact, as will be discussed below, the process[9] is quite stable. After typical runs of ~1 h to several hours, the cylinder is connected to a gas chromatograph to measure the H_2 content.

$CuAlO_2$ catalyst powders are prepared by solid-state reaction of CuO and Al_2O_3, followed by grinding between each calcining step for temperatures in the range of 800–1160 °C. X-ray diffraction (XRD) spectra of the final powder showed excellent agreement with the computed $CuAlO_2$ spectrum. The Brunauer-Emmett-Teller[10] (BET) surface area per gram of powder was found to be 22.7 m^2/g. The helium pycnometer[11] powder mass density was found to be 5.33×10^6 g/m^3. These two measurements imply an average particle diameter of 49.4 nm, consistent with the XRD grain size of 30–60 nm.

It has been found (see, e.g., Refs. 12 and 13) that $CuAlO_2$ band gaps can depend on material processing parameters. For that reason, we carried out optical-absorption experiments on thin films of the $CuAlO_2$ catalyst powders used in the H_2 generation experiments reported here. The films were formed by deposition onto a quartz slide from the catalyst water slurry. Following Pankov,[14] the direct and indirect band gaps are obtained from the absorption coefficient σ as shown in Fig. 2. For our $CuAlO_2$ powder the direct gap is found to be 3.01 eV, while the indirect gap is 1.87 eV. Thus both gaps are accessible by solar radiation. Exciting an electron across the indirect gap requires the assistance of a phonon for bulk materials. One might expect indirect-gap transitions to be more likely for the smaller catalyst nanoparticles or for higher temperatures.

Photocatalytic H_2 generation has been reported[5] for $CuAlO_2$ in water doped with sulfides and at a temperature of 321 K. Those authors[5] found, disappointingly, that the H_2 generation tends to zero after 20–30 min of run time.

Our experimental setup used a 0.2 g batch of $CuAlO_2$ powder mixed as a slurry with 170 ml of undoped, filtered, deaerated, and de-ionized (18 MΩ resistivity) water. For the temperature range of our data, 460–510 K (187–237 °C), the water is boiling. This vigorously stirs the water/catalyst slurry, eliminating a need for mechanical stirring. Note that this is just an oxide in water, containing no electrodes or

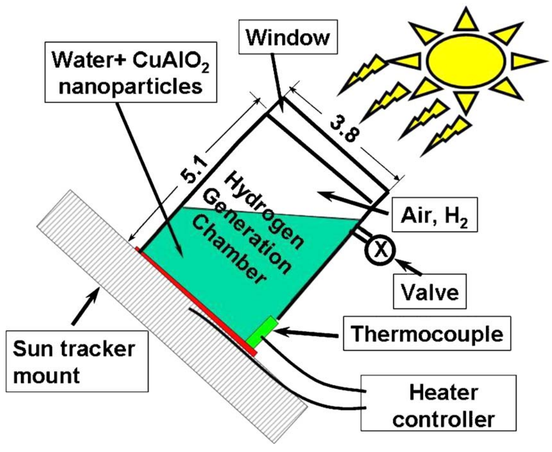

FIG. 1. (Color online) Schematic of the hydrogen generation apparatus. Dimensions are in centimeters.

1098-0121/2009/79(4)/041403(4)

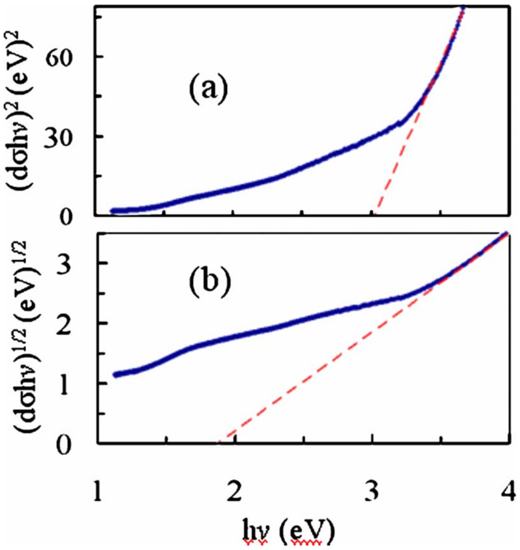

FIG. 2. (Color online) Determination of the band gaps for our $CuAlO_2$ powder thin films via optical-absorption experiments. Here σ is the absorption coefficient for a film of thickness d. Part (a) is for the direct allowed gap and part (b) for the indirect allowed gap.

chemicals. As such, one would expect the catalyst to be stable. Concentrations of hydrogen gas in units of ppm were determined after each generation run by connecting through the valve shown in Fig. 1 to a gas chromatograph containing a pulsed discharge H_2 detector.

Results are found in Fig. 3, a plot of ln R, where R is the hydrogen generation rate in ppm/h, versus $1/kT$ in units of 1/eV, where T is the water temperature. All data shown are taken from experiments using the same 0.2 g catalyst batch. Run times at each temperature varied from 0.42 to 4.03 h for data taken over a period of 2 months. During that 2 month time period, no decay of the H_2 generation rate was seen for any given temperature, so one can conclude that the process and catalyst are stable. This is consistent with powder x-ray spectra of the powder used in the experiment being unchanged over the 2 month period. These generation data were found to be typical of our data from other powder batches. The hydrogen generation rates of Fig. 3 increased from 715 to 6244 ppm/h as the temperature rose from 460 to 510 K. The error bars for these data are less than or approximately equal to the height of the symbols of Fig. 3. One can also see from Fig. 3 that the hydrogen generation rate R versus the water temperature T is accurately of the Arrhenius form,

$$R = (\nu_0/2) N_H \exp(-E_D/kT), \tag{1}$$

where the linear fit (correlation coefficient=0.98) yields $E_D = 0.94$ eV and $\ln(\nu_0 N_H/2) = 30.06$. Here one can consider E_D to be the H_2 desorption barrier per H atom, ν_0 is the desorption barrier approach frequency, and N_H is the total number of H atoms involved in the desorption process.

Interestingly, the thermal and photocatalytic effects are coupled. For example, in darkness at $T=473$ K ($1/kT = 24.6\ \mathrm{eV}^{-1}$), the experimental H_2 generation rate was lower than our measurement error, <100 ppm/h. This is to be compared to our measured H_2 generation rate of 780 ppm/h in the presence of sunlight at $T=473$ K (see Fig. 3).

The efficiency η of conversion of solar energy to chemical energy can be determined. Each H_2 molecule produced can liberate[15] a heat of formation $\varepsilon \approx 2.96$ eV by interaction with oxygen to form liquid water $[H_2(g) + 1/2 O_2(g) = H_2O(l)]$. η is the rate of production of this chemical energy per unit area of the Earth's surface divided by the total intensity of solar radiation. The efficiency is of the form $\eta = \varepsilon RV/AI$. This can be determined for our experimental system (Fig. 1) from the measured rate of H_2 generation R (Fig. 3), the measured chamber gas volume $V = 14.47\ \mathrm{cm}^3$, the area A of the window, and the measured solar intensity I for the data of Fig. 4 ($\sim 500\ \mathrm{W/m^2}$ over 300–800 nm). Solar flux intensities were measured using an Atlas Xenocal meter. For example, a chemical energy production rate of $5\ \mathrm{W/m^2}$ ($\eta = 1\%$) requires a solar H_2 generation rate of $0.063\ \mathrm{mol/h\ m^2}$ of Earth's surface.

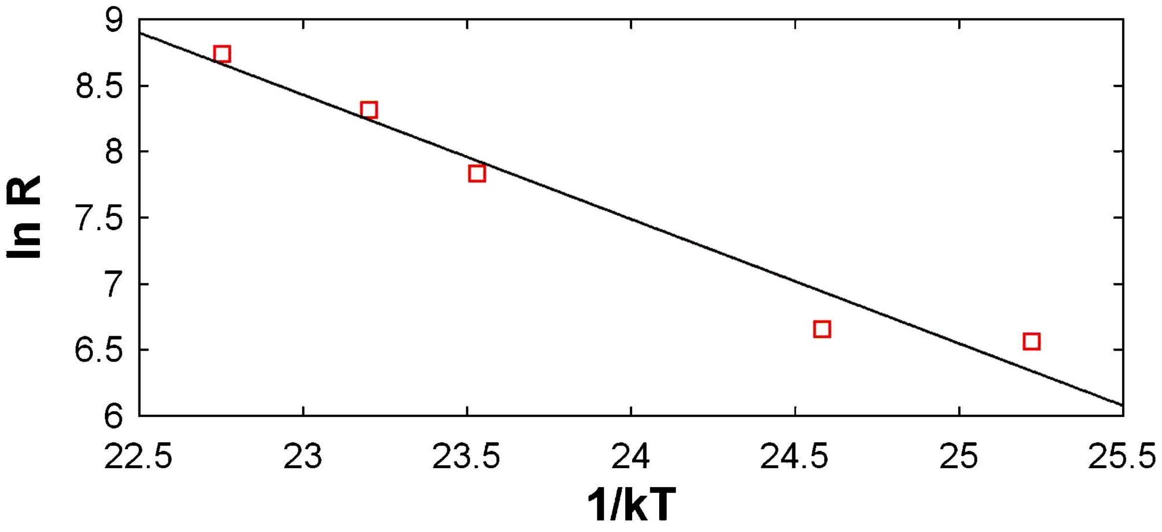

FIG. 3. (Color online) An Arrhenius plot of ln R versus $1/kT$, where R is the measured hydrogen gas generation rate in units of ppm/h at water temperature T, and kT is in units of 1/eV.

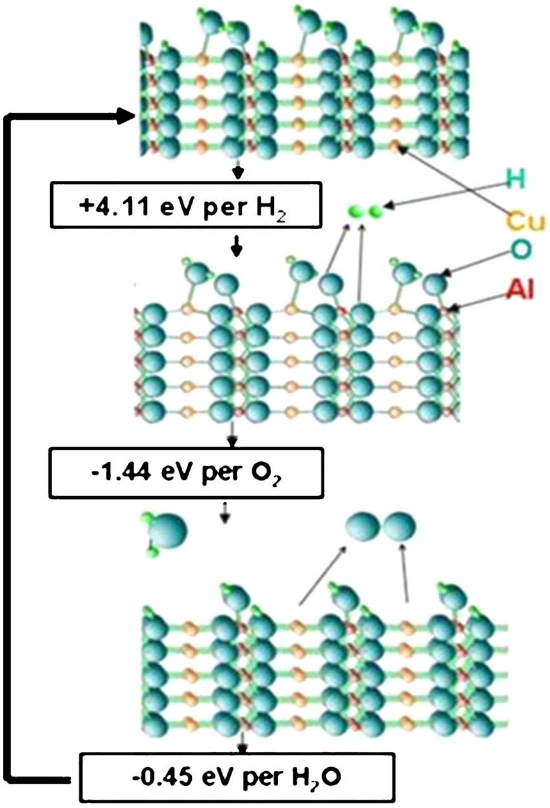

FIG. 4. (Color online) Schematic showing the results of first-principles computations of the H_2 and O_2 production cycle. H_2O molecules adsorb on the (110) surface of $CuAlO_2$ to produce gaseous H_2 and O_2 as described in the text.

From Eq. (1), one sees that the efficiency η depends exponentially on T through the generation rate R. Considering how well the data follow the Arrhenius line, especially at larger T, it is tempting to extrapolate to estimate the T required for a given efficiency η. It is found that for, e.g., $\eta = 10\%$, $T = 672$ K (=399 °C). At these higher temperatures, H_2O vapor pressures would be too high against the window of our current system. We are in the process of redesigning our hydrogen generation chamber (Fig. 1) in order to reach ~400 °C.

This temperature of 399 °C may be compared, e.g., with those in the range of 800–1300 °C required for solar water splitting with active redox reagent powders,[7] 800–900 °C required for thermocatalytic H_2 production from methane,[16] and 2000–2200 °C required for ZnO/Zn redox reactions[6] and direct thermal splitting.[8] It is expected that the significantly lower operating temperatures of the process described here will make the process easier to implement in a practical device.

How does one understand the results shown in Fig. 3? First-principles density-functional computations of the water splitting process on the surface of $CuAlO_2$ have been carried out[9] to help understand these processes. These computations are expected to yield the H_2 desorption barrier E_D in the absence of sunlight. Moreover, a better understanding of the water splitting process at the atomic level will ensue.

Density-functional computations for Fig. 4 were done by employing the plane-wave method[17] with ultrasoft pseudopotentials.[18] For the total-energy and force calculations, the exchange-correlation potential follows the generalized gradient approximation[19] (GGA), the primary approximation of the method, to solve the Kohn-Sham equations. Details of our application of the density-functional computational method are discussed in Ref. 20.

Computational results are shown in Fig. 4 for the energetics of water interacting with the $CuAlO_2(110)$ surface in the absence of illumination (darkness). The top image shows the water/$CuAlO_2$ interface at the atomic level and in the ground state. Note that the H_2O molecules adsorbed on the Al atoms dissociate, forming an OH ion on the Al atom and contributing a H atom to the neighboring O atom of the $CuAlO_2$ surface, thereby forming a second OH ion. H_2O molecules adsorbed on the Cu atoms do not dissociate at this point. The middle image is a snapshot of the desorbing H_2 coming from the dissociated H_2O, with a computed H desorption energy $E_H = 2.05$ eV. Subsequently, the H_2O adsorbed on the Cu atoms dissociate, filling the H atom vacancies caused by the H_2 desorption and leaving O atoms adsorbed on the Cu atoms. The bottom image is of these O atoms desorbing, with the O desorption energy $E_O = -0.72$ eV. Note that E_O being negative indicates O desorbs exothermically. Finally,[21] the catalyst surface returns to its original state (top image) by H_2O adsorbing on the Cu atoms, with a H_2O desorption energy $E_{H_2O} = 0.45$ eV.

Note that H_2 and O_2 were produced in this cycle by splitting H_2O, requiring a net $2E_H + E_O - E_{H_2O} = 2.94$ eV/H_2O molecule split. This sum of computed desorption energies is consistent with the measured[15] H_2O heat of formation of 2.96 eV. One can also determine an approximate H desorption energy E_H from the experimental[22] gaseous OH dissociation energy $E(OH)$ of 4.39 eV and a gaseous H_2 dissociation energy[23] $E(H_2)$ of 4.52 eV, with the assumption that the energy to desorb a H from a surface OH bond is $E_H \cong E(OH) - E(H_2)/2 = 2.13$ eV. The reason this simple approximation agrees reasonably well with our first-principles results is that the OH bonds in the gas and on the surface are relatively well localized in space and therefore similar. For example,[24,25] the vibrational frequency for a surface O-H is 1.11×10^{14}/s and in pure water it is 1.12×10^{14}/s.

The relatively large $E(OH)$ is what makes splitting H_2O so difficult. We saw earlier that there was clear experimental evidence of a beneficial coupling between photocatalytic and thermal effects. This is consistent with our measured H_2 desorption barrier per H atom, $E_D = 0.94$ eV, being well less than the experimental[22] OH dissociation energy of ~4.39 eV and the computed (dark) desorption energy $E_H = 2.05$ eV. This suggests that the solar radiation has created excited complexes $(OH)^*$, which require significantly less thermal energy to dissociate than the ground-state OH. This photocatalytic creation of $(OH)^*$ and subsequent thermal dissociation involves a coupling of thermal and photoelectric effects.

The ultraviolet and visible components of the solar spectrum contribute to the creation of $(OH)^*$, while ultraviolet, visible, and infrared components all raise the system temperature to contribute to the thermal dissociation. One mechanism for creating an $(OH)^*$ would be the photoexcitation of an OH bonding electron from the valence band to a conduction band (electron-hole pair). This conduction band may be a bulk catalyst band and/or an empty water/catalyst interfacial state band in the bulk band gap. The (OH)* could also be formed by a different process. The solar radiation will create electron-hole pairs in the $CuAlO_2$ catalyst. OH bonds typically have a net negative charge, which will tend to attract the hole of the electron-hole pair. If the hole was then to migrate to the OH bond and the electron of the electron-hole pair was to follow the hole to that site, it could produce an (OH)* like that created via a direct photoexcitation of an OH bonding electron. This migration to the catalyst surface would be limited by electron-hole recombination in the $CuAlO_2$ bulk. Regardless of how the (OH)* is formed, its OH bond would be expected to be significantly weakened by excitation of the bonding electron out of its ground-state configuration.

The (OH)* could, in principle, be modeled by density-functional theory. Here we have presented only ground-state (no sunlight) interfacial results for the process of splitting OH. (OH)* would require extending these computations to include photoexcited electronic states. Then modeling the coupling between thermal and photoelectric effects would require an additional computation of the difference in the thermal-desorption barrier E_D for (OH)* and OH.

In summary, a thermal-photocatalytic process for the generation of H_2 over $CuAlO_2$ nanoparticle catalysts in water and in the presence of natural sunlight is reported. Stable generation rates at each temperature are observed for a given catalyst sample for run times of ~ 1 h to several hours during experiments conducted over a 2 month period. Measured rates increased rapidly with temperature, and extrapolated rates suggest a 10% efficiency at 399 °C. This temperature is significantly less than those of solar thermal process for H_2. Moreover, the environment of $CuAlO_2$ in H_2O in our experiments is not corrosive. The measured value of the thermal activation barrier is 0.94 eV. First-principles computations indicate that H_2 desorption is the only energetically "uphill" step in the H_2 generation process. A H_2 generation process was proposed in which the H_2 is thermally desorbed, aided by a lowering of the desorption barrier due to solar radiation. In this way, the ultraviolet, visible, and infrared components of the solar spectrum can all contribute to H_2 generation.

---

[1] M. Grätzel, Nature (London) **414**, 338 (2001).

[2] A. Fujishima and K. Honda, Nature (London) **238**, 37 (1972).

[3] See, e.g., Z. Zou, J. Ye, K. Sayama, and H. Arakawa, Nature (London) **414**, 625 (2001).

[4] A. Kudo, Int. J. Hydrogen Energy **31**, 197 (2006).

[5] N. Koriche, A. Bouguelia, A. Aider, and M. Trari, Int. J. Hydrogen Energy **30**, 693 (2005).

[6] See, e.g., A. Steinfeld, Int. J. Hydrogen Energy **27**, 611 (2002).

[7] C. Agrafiotis, M. Roeb, A. G. Konstandopoulos, L. Nalbandian, V. T. Zaspalis, C. Sattler, P. Stobbe, and A. M. Steele, Sol. Energy **79**, 409 (2005).

[8] A. Kogan, Int. J. Hydrogen Energy **23**, 89 (1998) directly splits H_2O at temperatures up to 2500 °C.

[9] J. R. Smith, T. J. Van Steenkiste, and X.-G. Wang, U.S. Patent Application No. 0196268A1 (2007) and additional pending patent applications.

[10] See, e.g., Terrell L. Hill, Proc. Natl. Acad. Sci. U.S.A. **93**, 14328 (1996).

[11] See, e.g., W. B. Lievers, V. Lee, S. M. Arsenault, S. D. Waldman, and A. K. Pilkey, J. Biomech. **40**, 1903 (2007).

[12] R.-S. Yu, S.-C. Liang, C.-J. Lu, D.-C. Tasi, and F.-S. Shieu, Appl. Phys. Lett. **90**, 191117 (2007).

[13] J. Pellicer-Porres, A. Segura, A. Munoz, P. Rodriguez-Hernandez, D. Kim, M. S. Lee, and T. Y. Kim, Appl. Phys. Lett. **88**, 181904 (2006).

[14] J. I. Pankov, *Optical Processes in Semiconductors* (Prentice-Hall, Englewood Cliffs, NJ, 1971).

[15] The heat of formation of liquid $H_2O(l)$ from gaseous $O_2(g)$ and $H_2(g)$ has been accurately known for many years. See, e.g., F. D. Rossini, Proc. Natl. Acad. Sci. U.S.A. **16**, 694 (1930), where it is reported to be 2.96 eV/H_2O molecule (285.89 kJ/mol) at 25 °C.

[16] K. K. Lee, G. Y. Han, K. J. Yoon, and B. W. Lee, Catal. Today **93-95**, 81 (2004).

[17] G. Kresse and D. Joubert, Phys. Rev. B **59**, 1758 (1999).

[18] D. Vanderbilt, Phys. Rev. B **41**, 7892 (1990).

[19] J. P. Perdew, K. Burke, and M. Ernzerhof, Phys. Rev. Lett. **77**, 3865 (1996).

[20] X. G. Wang, J. R. Smith, and A. G. Evans, Phys. Rev. B **74**, 081403(R) (2006).

[21] A movie of the computed dynamics of this process is available on request.

[22] *CRC Handbook of Chemistry and Physics*, 59th ed., edited by B. R. C. Weast (CRC, Boca Raton, FL, 1979), p. D-46.

[23] *CRC Handbook of Chemistry and Physics*, 69th ed., edited by B. R. C. Weast (CRC, Boca Raton, FL, 1989), p. F-176.

[24] K. C. Hass, W. F. Schneider, A. Curionl, and W. Andreoni, Science **282**, 265 (1998).

[25] X. G. Wang and J. R. Smith, Phys. Rev. B **70**, 081401(R) (2004).